J Mol Model (2005) 12: 16–23
DOI 10.1007/s00894-005-0280-7

ORIGINAL PAPER

Ricardo O. Freire · Fabiana R. Gonçalves e. Silva
Marcelo O. Rodrigues · Maria E. de. Mesquita
Nivan B. da Costa. Jùnior

Design of europium(III) complexes with high quantum yield

Received: 27 October 2005 / Accepted: 12 April 2005 / Published online: 26 July 2005

Abstract This work describes a rational planning of a new light-conversion molecular device with high quantum yield. For this, we made modifications in the 3-amino-2-carboxypyridine and 3-amino-2-carboxypirazine acid ligands, generating eight different complexes. Theoretical methods have been used to calculate the quantum yield of each of the complexes. We first used the Sparkle model to calculate the ground-state geometries of the eight complexes. These data were used to perform theoretical predictions of the energy transitions using the INDO/S–CI method. After having obtained the geometry and the energy transitions, the energy transfer rates and quantum yield were calculated using a theoretical approach based on the application of the 4f–4f transition theory. The results show that the modifications in the 3-amino-2-carboxypyridine ligand had generated three complexes with high quantum yield (about 52.8, 51.6 and 52.8%). On the other hand, the modifications in the 3-amino-2-carboxypirazine led to only one complex with quantum yield larger than 50%, but it is the most efficient complex projected.

Keywords Sparkle model · Europium complexes · Quantum yield

R. O. Freire (✉)
Departamento de Química Fundamental, UFPE,
50590-470 Recife, PE, Brazil
E-mail: rfreire@ufpe.br
Tel.: +55-81-2126-8447
Fax: +55-81-2126-8442

M. O. Rodrigues · M. E. Mesquita · N. B. C. Jùnior
Departamento de Química, UFS,
49100-000 São Cristóvão, SE, Brazil

F. R. G. Silva
Departamento de Química, UFRN,
59078-970 Natal, RN, Brazil

Introduction

The design of efficient light-conversion molecular devices (LCMDs) based on lanthanide complexes have been studied by several research groups [1–11]. The reason for so much interest is the great applicability of these devices as contrast agents in magnetic-resonance imaging techniques (MRI) [12–15] such as luminescent labels in fluoroimmunoassays [2, 16–19]; LCV dosimeters [20] and thin-film electroluminescent devices [21], among others.

Obtaining efficient LCMDs is not a simple task. The design of the complexes with high quantum yield is directly related to the understanding of each of the stages involved in the luminescence process of these complexes. In the first stage, the light in the UV regions is absorbed by the ligands, which is why they are chosen by absorption intensity. In the second stage, the energy is transferred from the triplet state of the ligand to the excited state of the lanthanide ion. When the triplet state of the ligands is resonant with one of the excited states of the lanthanide ion, in general, the ligands-ion energy transfer is intense. In the last stage, the excited lanthanide ion decays to the ground state and most of the energy must be emitted via photon emission in the visible region [22].

For some applications, the ligands chosen should have specific properties. For example, water-soluble ligands are the choice suitable for the analysis of biological systems.

The theoretical models developed by our group for predicting the details of each one of these stages have been used with success [11, 23–26]. Recently, we published a new version of the Sparkle model [27]. We used this model to calculate the ground state geometry of Eu(III) complexes [28, 29]. This is the first step for starting the design of new LCMDs. The energy-transfer rates and quantum yield were determined by means of a theoretical approach based on the application of the 4f–4f transition theory [30].

The purpose of the present work is to find a new complex with high quantum yield. For this we used the theoretical models described below for studying lanthanide coordination complexes with ligands derived from 3-amino-2-carboxypyridine and 3-amino-2-carboxypirazine. This procedure has already been used successfully in the prediction of the quantum yield of other europium complexes. In recent work [23], the quantum yield was calculated for the $Eu(fod)_3phen$–NO complex. The calculated value, 41%, agrees well with the experimental observed value, 43%.

Theoretical details

Sparkle model

In this model we postulate that the lanthanide ion can be represented satisfactorily by the Coulombic potential corresponding to a point charge of value identical to its oxidation state, superimposed by a repulsive exponential potential, both centered in the position of the nucleus of the lanthanide ion [27]. This model gives good results because the overlap between the 4f orbitals of the lanthanide ion and the orbitals of the ligand atoms is very small, conferring to the chemical bond (lanthanide–ligand) largely electrostatic character.

In the newest version of our Sparkle model, SMLC II [27], we sought to improve the Sparkle model, in various ways: (1) by including the europium atomic mass, (2) by reparameterizing the model within AM1 for a new response function, including all distances of the coordination polyhedron for tris(acetylacetonate)(1,10-phenanthroline) Eu(III), (3) by implementing the model in the software package MOPAC93r2 [31] and (4) by including spherical Gaussian functions in the expression that computes the core–core repulsion energy. All these modifications have considerably improved the Sparkle model.

In recent work, we analyzed the efficacy of the Sparkle model compared to ECP ab initio calculations [32]. The results show that the calculation of the ground state geometries of Eu(III) complexes can be carried out using the Sparkle model with satisfactory accuracy and low CPU time.

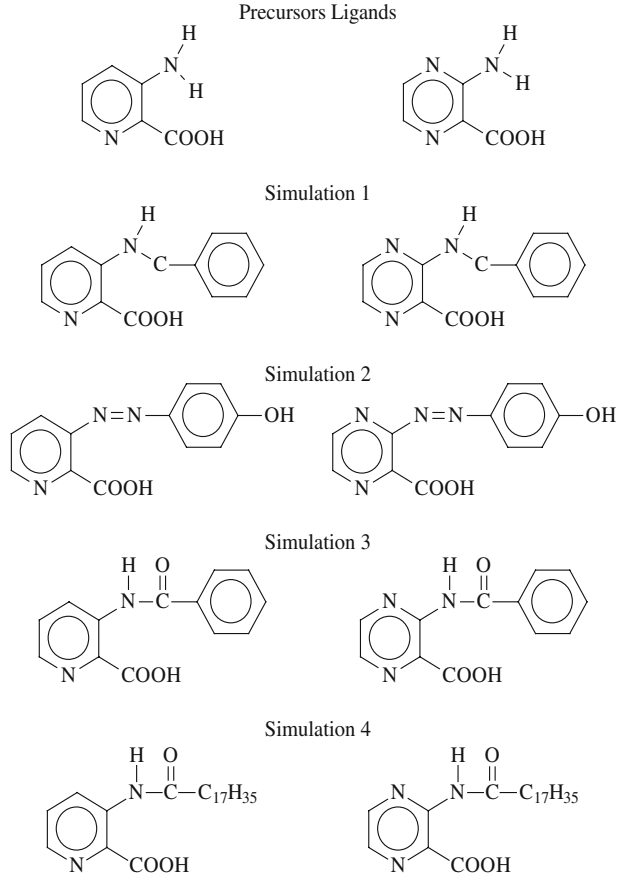

Fig. 1 Schematic two-dimensional representation of the modified ligands that have been used in the design of the new LCMD

The energy transfer rates and quantum yield

The models used to obtain the energy transfer rates between the ligands and the lanthanide ion, the numerical solution of the rate equations and the emission quantum yield are described in Refs. [30, 33, 34].

Methodology

Design of the LCMD

The design of the new complex was made by modifying the 3-amino-2-carboxypyridine acid and 3-amino-2-carboxypirazine acid ligands. In the first simulation, the objective was to analyze the effect of changing of the amine group to an amide group. In the other simulations larger groups such as benzoyl chloride, were connected to the amide to diminish the complex polarity and increase the solubility in organic solvents. Figure 1 shows the modified ligands that had been used in the design of the new LCMD.

Geometry optimization and calculation of the transition energies

The complexes studied are composed of three ligands and two water molecules coordinated to the lanthanide ion–$Eu(L)_3{\cdot}2H_2O$, where L are the modified ligands shown in Fig. 1. The ground-state geometry of the eight complexes was calculated with the Sparkle model using the MOPAC93r2 package [31]. The MOPAC keywords used in all Sparkle/AM1 calculations were: GNORM = 0.25, SCFCRT = 1D − 10 (in order to increase the SCF convergence criterion) and *XYZ* (the geometry optimizations were performed in Cartesian coordinates). The

intermediate neglect of differential overlap/spectroscopic–configuration interaction (INDO/S–CI) method [35, 36] implemented in the ZINDO program [37] was used to calculate the transition energies of the Eu(III) complexes. The CIS space was gradually increased until there were no further meaningful changes in the calculated transitions.

Ligand–lanthanide ion energy transfer and quantum yield

Some restrictions were taken into account in the calculation of the energy-transfer rates and in the emission quantum yields. These restrictions were based on experimental data (electronic spectra and energy transfer rate) taken from several lanthanide compounds found in the literature. Such restrictions were necessary because the electronic spectra calculations generally provide too

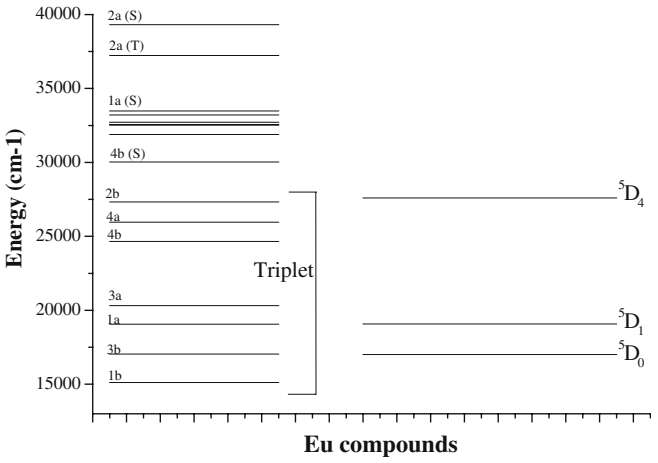

Fig. 2 Diagram relating the singlet and triplet levels of the eight ligands studied with the emitting level $^5D_0$, $^5D_1$ and $^5D_4$ of the lanthanide ion

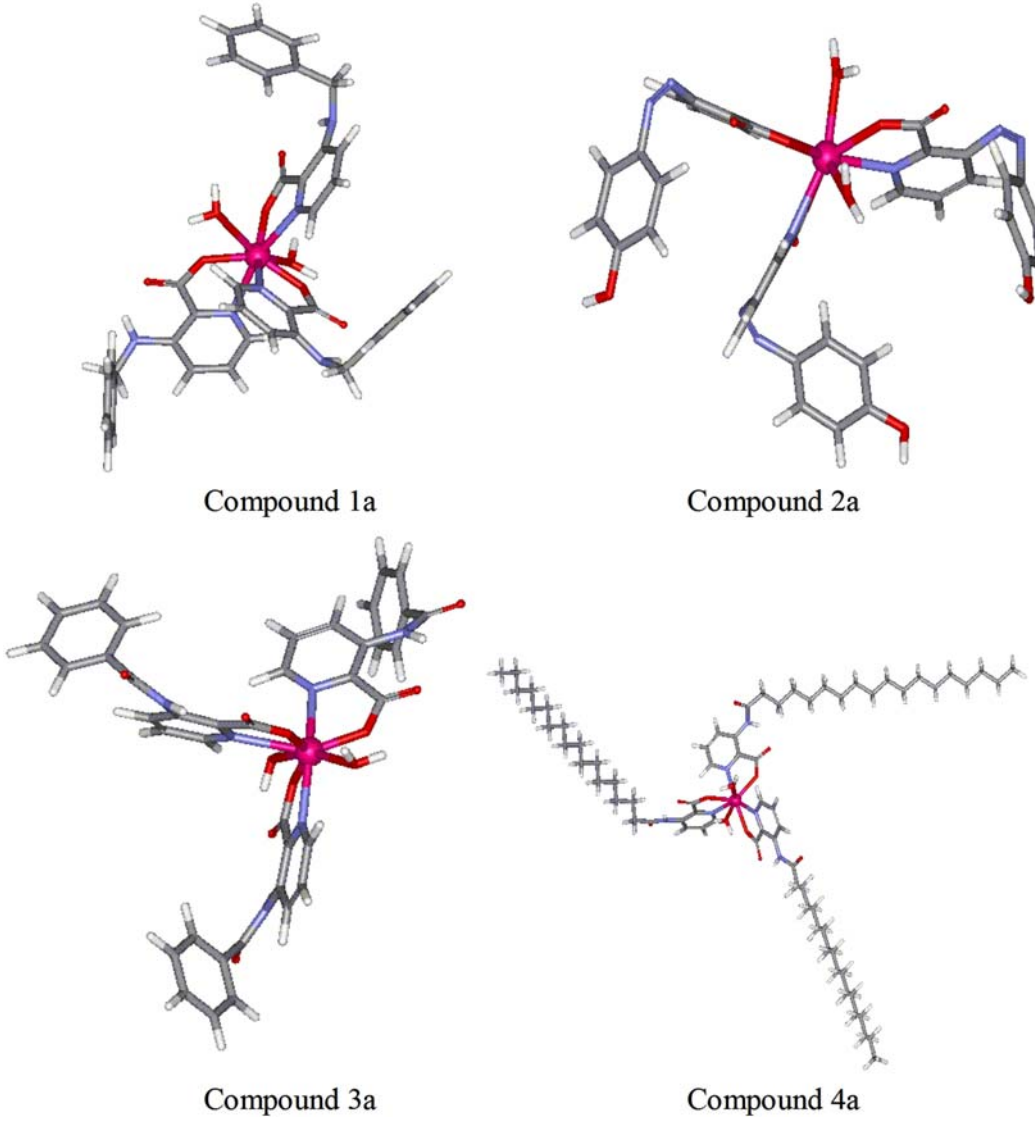

Fig. 3 Calculated ground state geometry of the four complexes with ligands derivatives of 3-amino-2-carboxypyridine acid

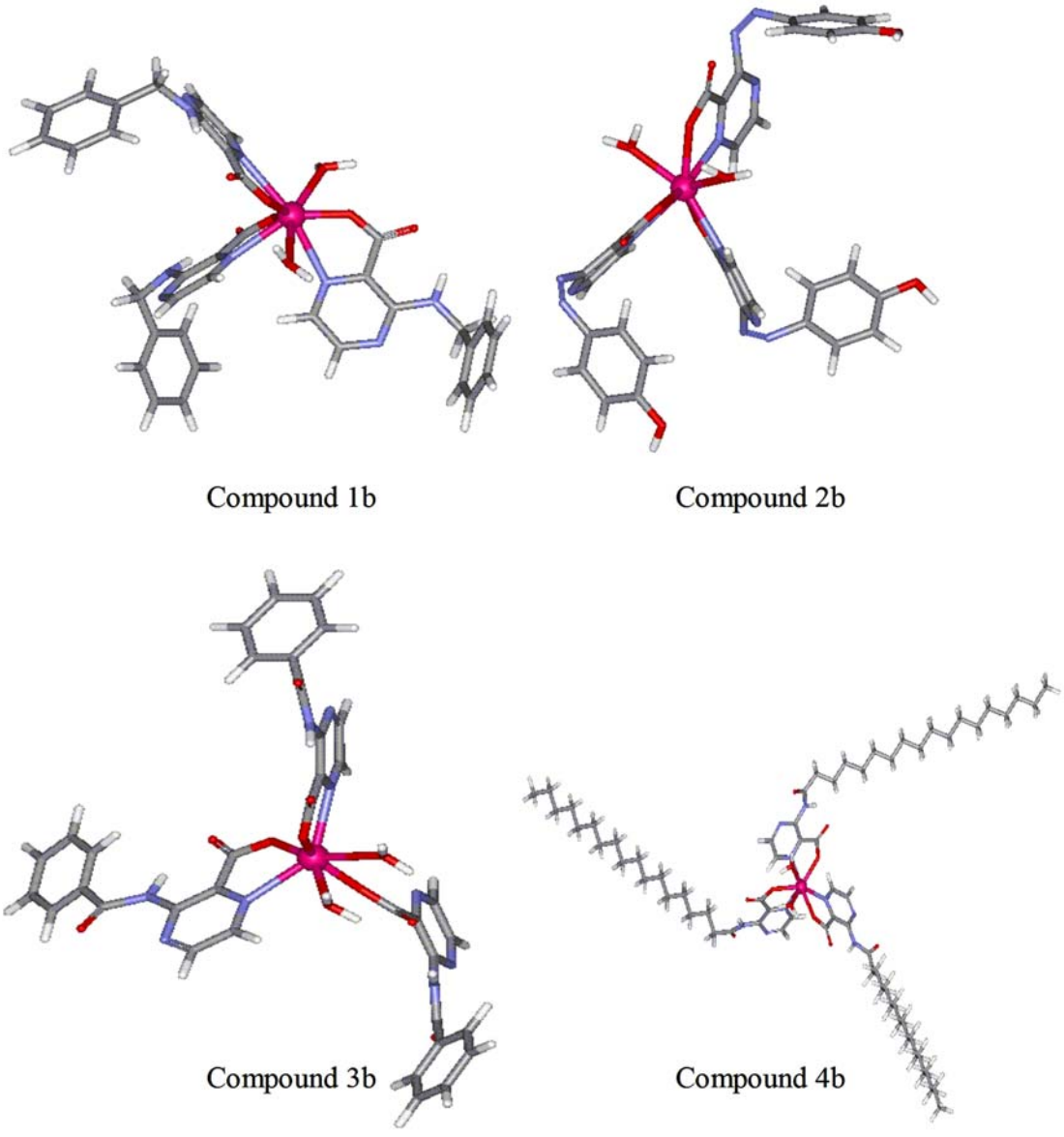

Fig. 4 Calculated ground state geometry of the four complexes with ligands derivatives of 3-amino-2-carboxypirazine acid

much data, which create complications in posterior analyses. These restrictions were:

1. The oscillator strength of the singlet states must be larger than 0.2.
2. Only the triplet state of lowest energy was considered, which is related to the singlet state chosen in item 1.
3. The singlet state must have energy below 40.000,00 cm^{-1} .
4. In the calculation of the energy-transfer rate, the singlet (S) or triplet (T) states and the $^5 D_0$ or $^5 D_1$ levels should present energy difference $\Delta E = E(\text{S or T}) - E(^5 D_j)$ below 9,000 cm^{-1} .

In the study of the energy-transfer process of the ligand ⇒ lanthanide, the energy diagram shown in Fig. 2 was used. For compound **2a**, item (4) of the restrictions was taken into consideration. Only the five energy levels S_0, S, T, $^5 D_4$ and $^5 D_0$ were considered. In the study of the other compounds, these five levels and also the $^5 D_1$ energy level were considered. With the above restrictions, energy transfer involving the triplet state and the $^5 D_0$ and $^5 D_1$ levels was obtained only for the **1a**, **1b**, **3a**, **3b** and **4b** compounds, because the **2b**, **2a** and **4a** compounds have energy differences between the donor and acceptor states larger than 9,000 cm^{-1} . The transfers involving the triplet state and the $^5 D_4$ level were calculated only for the **2a**, **2b** and **4a** compounds because of a good resonance condition between these states.

Results

The geometries calculated for the Sparkle model are shown in Figs. 3 and 4. Figure 3 shows the optimized

geometries of the four complexes with ligands derivatives of 3-amino-2-carboxypyridine acid and the optimized atomic coordinates for the coordination polyhedron of the complexes are shown in Table 1. The coordination polyhedron of each complex is formed by the nitrogens and oxygens of the three modified ligands and two oxygens (O8, O9) from the water molecules.

Figure 4 shows the optimized geometries of the four complexes with ligands derivatives of 3-amino-2-carboxypirazine acid. Table 2 presents the optimized atomic coordinates for the coordination polyhedron of the complexes. In this case, the atoms of the coordination polyhedron are ordered in the same way as in Table 1.

The parameters obtained from the Sparkle model and INDO/S–CI used in the energy transfer rate calculation are given in Table 3. These parameters are the singlet and triplet-energy positions (medium value), the value of the R_L and the transition moment. The parameters $\gamma_{triplet}$ (triplet state bandwidth), A_{rad} (taken as the sum of the spontaneous emission coefficients of the transitions $^5D_0 \rightarrow {}^7F_{0,1,2,4}$) and τ^{-1} ($^5D_0$) (emitter level lifetime) used in the calculation of the emission quantum yield were obtained from the electronic spectra of a compound similar to the one analyzed in this work [38].

Table 1 Interatomic distances for the coordination polyhedron of the four complexes with ligands derivatives of 3-amino-2-carboxypyridine acid

Atoms	*X* (Å)	*Y* (Å)	*Z* (Å)	*X* (Å)	*Y* (Å)	*Z* (Å)
	Compound **1a**			Compound **2a**		
Eu(III)	0.0000	0.0000	0.0000	0.0000	0.0000	0.0000
N2	−1.9060	1.1350	−1.1380	2.5270	0.0000	0.0000
N3	−1.2910	0.9030	2.1330	−0.7880	2.4010	0.0000
N4	0.6550	−1.1970	−2.1950	0.4630	−2.0110	−1.4570
O5	1.1140	1.1790	−1.1730	0.2070	−2.0930	1.1020
O6	−1.5620	−1.2800	−0.1340	1.0710	0.9860	−1.8790
O7	1.0440	−0.2660	1.6680	−1.7550	0.5550	1.5050
O8	0.5060	−2.3820	0.5650	−2.1880	−0.5280	−0.8070
O9	0.3490	2.8020	0.4250	0.5630	0.1350	2.3250
	Compound **3a**			Compound **4a**		
Eu(III)	0.0000	0.0000	0.0000	0.0000	0.0000	0.0000
N2	−2.3400	1.1350	0.2710	2.5310	−0.0380	0.0720
N3	0.4570	1.2830	2.1600	−0.3800	2.4940	0.1940
N4	−0.1890	−0.3680	−2.4560	0.2950	0.5990	−2.4430
O5	0.2760	1.7380	−0.9510	−1.9820	0.2130	−1.3050
O6	−1.4170	−1.3190	0.4080	1.0620	−2.0990	−0.3440
O7	1.6750	−0.6450	0.8190	0.5700	1.0200	2.0660
O8	0.5940	−2.4470	−0.4300	−1.2820	−1.9810	−0.5830
O9	−0.3600	4.5600	−0.3840	−1.9950	−0.3740	1.2630

Table 2 Interatomic distances for the coordination polyhedron of the four complexes with ligands derivatives of 3-amino-2-carboxypirazine acid

Atoms	*X* (Å)	*Y* (Å)	*Z* (Å)	*X* (Å)	*Y* (Å)	*Z* (Å)
	Compound **1b**			Compound **2b**		
Eu(III)	0.0000	0.0000	0.0000	0.0000	0.0000	0.0000
N2	−2.0650	1.1510	−0.9690	2.5260	0.0000	0.0000
N3	−1.1930	0.9360	2.2400	−0.9020	2.3600	0.0000
N4	0.3310	−1.1460	−2.4470	0.5280	−1.9330	−1.5350
O5	1.0130	1.1200	−1.2730	0.2860	−2.1270	1.0170
O6	−1.5430	−1.2800	−0.0670	1.0730	1.1030	−1.8140
O7	1.0960	−0.2680	1.6230	−1.7540	0.4820	1.5330
O8	0.6750	−2.3200	0.3750	−2.1770	−0.5610	−0.8110
O9	0.3270	2.7710	0.3290	0.5740	0.0860	2.3240
	Compound **3b**			Compound 4**b**		
Eu(III)	0.0000	0.0000	0.0000	0.0000	0.0000	0.0000
N2	−1.9490	1.5430	0.5070	2.5300	−0.1020	0.0360
N3	0.3130	−2.9890	3.3310	−0.4510	2.4850	0.1720
N4	0.9290	−1.4330	−1.9670	0.2880	0.6440	−2.4320
O5	0.9830	1.1480	−1.2940	−1.9840	0.2020	−1.3060
O6	−1.6770	−0.8260	−0.6090	1.0120	−2.1100	−0.4260
O7	0.4590	−0.5880	1.8010	0.6850	1.0900	1.9950
O8	2.4920	0.1660	0.3890	−1.3380	−1.9700	−0.4820
O9	1.0130	1.9440	1.1320	−1.9910	−0.2680	1.2970

Table 3 Parameters obtained from the Sparkle model and INDO/S–CI used in the energy transfer rate calculation

Compound	Singlet states energy (cm^{-1}) (medium value)	Triplet state energy (cm^{-1})	R_L (singlet) (Å)	R_L (triplet) (Å)	Electric dipole matrix element (μ) (ues^2 cm^2)
1a	33,486	19,064	6.25	4.76	1.15×10^{-36}
2a	39,309	37,229	7.53	7.67	1.36×10^{-36}
3a	32,563	20,315	7.09	7.05	1.29×10^{-36}
4a	33,213	25,961	5.83	5.57	0.80×10^{-36}
1b	32,719	15,113	6.99	5.97	0.31×10^{-36}
2b	31,898	27,324	4.35	7.80	2.06×10^{-36}
3b	32,524	17,031	5.14	4.40	2.00×10^{-36}
4b	30,025	24,651	5.43	4.86	1.14×10^{-36}

Table 4 Calculated values for the energy transfer and back-transfer rates in **1a**, **2a**, **3a**, **4a**, **1b**, **2b**, **3b** and **4b** compounds

Ligand state (cm^{-1})		4f State (cm^{-1})	Transfer rate (s^{-1})	Back-transfer rate (s^{-1})
Compound **1a**				
Triplet	→	$^5D_0$ (17,300)	$k_{26} = 1.02 \times 10^7$	$K_{62} = 546$
Triplet	←	$^5D_1$ (19,070)	$K_{52} = 2.16 \times 10^8$	$k_{25} = 2.10 \times 10^8$
Singlet	→	$^5D_4$ (27,600)	$k_{34} = 1.36 \times 10^{5a}$	K_{43} is insignificant
Compound **2a**				
Triplet	→	$^5D_4$ (27,600)	$K_{24} = 1.08 \times 10^3$	k_{42} is insignificant
Singlet	→	$^5D_4$ (27,600)	$k_{34} = 535^a$	K_{43} is insignificant
Compound **3a**				
Triplet	→	$^5D_0$ (17,300)	$k_{26} = 1.09 \times 10^5$	$K_{62} = 0.015$
Triplet	→	$^5D_1$ (19,070)	$K_{25} = 2.71 \times 10^6$	$K_{52} = 7.19 \times 10^3$
Singlet	→	$^5D_4$ (27,600)	$k_{34} = 9.80 \times 10^{4a}$	K_{43} is insignificant
Compound **4a**				
Triplet	←	$^5D_4$ (27,600)	$k_{42} = 3.58 \times 10^5$	$K_{24} = 145.4$
Triplet	→	$^5D_1$ (19,070)	$K_{25} = 8.39 \times 10^6$	k_{52} is insignificant
Singlet	→	$^5D_4$ (27,600)	$k_{34} = 2.36 \times 10^{5a}$	K_{43} is insignificant
Compound **1b**				
Triplet	←	$^5D_0$ (17,300)	$k_{62} = 2.26 \times 10^5$	$K_{26} = 28.1$
Triplet	←	$^5D_1$ (19,070)	$K_{52} = 2.36 \times 10^6$	$K_{25} = 0.015$
Singlet	→	$^5D_4$ (27,600)	$k_{34} = 9.98 \times 10^{4a}$	K_{43} is insignificant
Compound **2b**				
Triplet	→	$^5D_1$ (19,070)	$k_{25} = 3.14 \times 10^5$	K_{52} is insignificant
Triplet	←	$^5D_4$ (27,600)	$K_{42} = 5.32 \times 10^4$	$k_{24} = 1.42 \times 10^4$
Singlet	→	$^5D_4$ (27,600)	$k_{34} = 2.39 \times 10^{6a}$	$K_{43} = 135$
Compound **3b**				
Triplet	→	$^5D_0$ (17,300)	$K_{26} = 4.46 \times 10^7$	$K_{62} = 3.84 \times 10^7$
Triplet	←	$^5D_1$ (19,070)	$K_{52} = 6.58 \times 10^8$	$k_{25} = 3.98 \times 10^4$
Singlet	→	$^5D_4$ (27,600)	$k_{34} = 6.87 \times 10^{5a}$	K_{43} is insignificant
Compound **4b**				
Triplet	→	$^5D_0$ (17,300)	$k_{26} = 1.98 \times 10^6$	K_{62} is insignificant
Triplet	→	$^5D_1$ (19,070)	$K_{25} = 1.15 \times 10^8$	k_{52} is insignificant
Singlet	→	$^5D_4$ (27,600)	$k_{34} = 1.09 \times 10^{6a}$	$K_{43} = 10.5$

[a] Dipole–dipole mechanism.

The following parameters were used: $\gamma_{triplet} = 4{,}000\ cm^{-1}$, $A_{rad} = 900\ s^{-1}$ and $\tau^{-1}(^5D_0) = 1{,}667\ s^{-1}$. A value of $10^6\ s^{-1}$ was assumed for all non-radiative decay rates among the 4f–4f transitions. The back-transfer rates were obtained by multiplying the energy transfer rate by the Boltzmann factor $e^{-|\Delta|/k_BT}$ at room temperature. The direct transfer rate to the $^5D_0$ level was calculated assuming a factor of thermal population equal to 0.17, at 300 K, for the $^7F_1$ manifold and the energy difference $\Delta E = E(\text{triplet}) - [E(^5D_0) - E(^7F_1)]$.

The energy-transfer and back-transfer rates calculated for the levels $^5D_0$, $^5D_1$ and $^5D_4$ of the lanthanide ion are given in Table 4. The exchange mechanism is the most efficient, being higher than the energy-transfer rates involving the level $^5D_1$ (about 10^6 –10^8 s^{-1}). The rates corresponding to the multipolar mechanism involving the level $^5D_4$ are relatively low (about 10^4 – 10^5 s^{-1}). However, they represent an efficient channel of

Table 5 Values of the emission quantum yield of the compounds

Compound	Quantum yield (%)
1a	52.80
2a	0.47
3a	51.60
4a	52.82
1b	$2.26 \times x10^{-4}$
2b	41.20
3b	1.00
4b	53.41
Compound	Quantum yield (%)
1a	52.80
2a	0.47
3a	51.60
4a	52.82
1b	$2.26 \times x10^{-4}$
2b	41.20
3b	1.00
4b	53.41

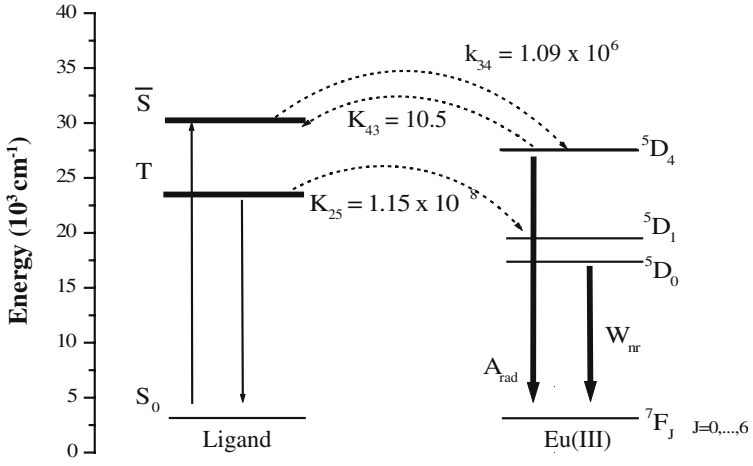

Fig. 5 Diagram of the most probable states to be involved in the energy transfer process in the compound **4b**. The rates W_{nr} and the A_{rad} represent non-radiative and radiative processes, respectively

population for the emitting level $^5D_0$, since that the back-transfer is small. Table 5 shows the quantum yields of the eight compounds.

Discussion

The compounds **1b** ($q = 2.26 \times 10^{-4}$ %), **2a** ($q = 0.47\%$) and **3b** ($q = 1\%$) are the ones that give the lowest quantum yield. The compounds **1b** and **3b** have the triplet state energy below the $^5D_0$ emitting level or resonant with it. This favors the energy transfer of the $^5D_0$ (emitting level of the lanthanide ion) to the triplet state, diminishing the emission quantum yield.

Compound **2a** gives a low quantum yield because it involves only the multipolar mechanism in the study of the energy transfer process, whose values of transfer rate are smaller than these obtained by the exchange mechanism. The exchange mechanism was not considered because the energy of the triplet state is very high, therefore excluding the appropriate conditions of resonance of this state with the levels $^5D_0$ and $^5D_4$.

Compound **4b** gave the highest quantum yield ($q = 53.41\%$). This compound is favored because the energy transfer rates to lanthanide levels W_{ET} ($T \rightarrow {}^5D_1$ and $S \rightarrow {}^5D_4$) are sufficiently high compared to the back-transfer rates, which are small. This happens because the singlet and triplet states are in an appropriate energy position, disfavoring the energy back-transfer. This is shown in Fig. 5. The energy-transfer rate between the singlet state and the $^5D_4$ level is 1.09×10^6 s^{-1} while the back-transfer rate is 10.5 s^{-1}. This can also be observed in the triplet state. The energy-transfer rates between the triplet state and the $^5D_1$ and $^5D_0$ levels are 1.15×10^8 s^{-1} and 1.09×10^6 s^{-1}, respectively, while the back-transfer rates are small.

The compounds that possess a triplet state below the $^5D_0$ or are resonant with the $^5D_0$ and $^5D_1$ levels are the ones that give the lowest quantum yield because the transfer rates $^5D_0$ or $^5D_1 \rightarrow T$ are high, making possible the depopulation of the emitting level of the lanthanide ion.

Conclusions

The design carried out indicates that the europium coordination complex **4b** gives the highest quantum yield, while the compound **1b** is one that gives the lowest quantum yield. These results are associated to the position of the triplet state and to the values of the energy transfer and back-transfer rates.

Our group is synthesizing the lanthanide complexes that present the highest and lowest emission quantum yields.

Supplementary material

Optimized geometries of the eight complexes with ligands derivatives of 3-amino-2-carboxypyridine acid and 3-amino-2-carboxypirazine acid, respectively. This material is available free of charge via the Internet.

Acknowledgements The authors thank FAP (state agency) and CNPq (Brazilian agency), CAPES (Brazilian agency), for financial support.

References

1. Sabbatini N, Guardigli M, Manet I, Ungaro R, Casnati A, Ziessel R, Ulrich G, Asfari Z, Lehn J-M (1995) Pure Appl Chem 67:135–140
2. Mathis G (1995) Clin Chem 41:1391–1397
3. Mikola H, Takkalo H, Hemmila I (1995) Bioconjug Chem 6:235–241
4. Piguet C, Bernardinelli G, Hopfgartner G (1997) Chem Rev 97:2005–2062
5. Werts MHV, Hofstraat JW, Geurts FAJ, Verhoeven JW (1997) Chem Phys Lett 276:196–201
6. Nassar EJ, Calefi PS, Rosa ILV, Serra AO (1998) J Alloys Comp 277:838–840
7. Petoud S, Bunzli J-CG, Schenk KJ, Piguet C (1997) Inorg Chem 36:1345–1353
8. Wolbers MPO, van Veggel FCJM, Snellink-Ruel BHM, Hofstraat JW, Geurts FAJ, Reinhoudt DN (1997) J Am Chem Soc 119:138–144

9. Parker D, Kanthi-Senanayake P, Williams JAG (1998) J Chem Soc Perkin Trans II:2129–2139
10. Oude Wolbers MP, van Veggel FCJM, Snellink-Ruel BHM, Hofstraat JW, Geurts FAJ, Reinhoudt DN (1998) J Chem Soc Perkin Trans II:2141–2150
11. de Sa GF, Malta OL, Donega CD, Simas AM, Longo RL, Santa-Cruz PA, da Silva EF (2000) Coord Chem Rev 196:165–195
12. Partain L, James AE, Rollo FD, Price RR (1983) Nuclear magnetic resonance (NMR) imaging. WB Saunders, Philadelphia
13. Lauffer RB (1987) Chem Rev 87:901–927
14. Tweedle MF, Bünzli JCG, Choppin GR (1989) Chemical and earth science. Elsevier, Amsterdam
15. Kumar K, Tweedle MF (1993) Pure Appl Chem 65:515–520
16. Hemmila IA (1991) Applications of fluorescence in immunoassays. Wiley, New York
17. Bunzli J-C, Choppin GR (1989) Medical and environmental science. Elsevier, Amsterdam
18. Soukka T, Antonen K, Härmä H, Pelkkikangas A-M, Huhtinen P, Lövgren T (2003) Clin Chim Acta 328:45–58
19. Taylor DL, Waggoner AS, Murphy RF, Lanni F, Birge RR (1986) Applications of fluorescence in biomedical sciences. AR Liss, New York
20. Gameiro CG, da Silva EF Jr, Alves S Jr, de Sá GF, Santa-Cruz PA (1999) Mater Sci Forum 315:249–256
21. Kido J, Ikeda W, Kimura M, Nagai K (1996) Jpn J Appl Phys 35:394–396
22. Sabbatini N, Guardigli M, Lehn J-M (1993) Coord Chem Rev 123:201–228
23. de Mesquita ME, Junior SA, da Costa NB, Freire RO, Gonçalves e Silva FR, de Sá GF (2003) J Solid State Chem 171:183–188
24. Faustino WM, Rocha GB, Gonçalves e Silva FR, Malta OL, de Sá GF, Simas AM (2000) J Mol Struct (THEOCHEM) 527:245–251
25. de Mesquita ME, Gonçalves e Silva FR, Albuquerque RQ, Freire RO, da Conceição EC, da Silva JEC, Júnior NBC, de Sá GF (2004) J Alloys Compd 366:124–131
26. de Mesquita ME, Junior AS, Gonçalves e Silva FR, Couto dos Santos MA, Freire RO, Júnior NBC, de Sá GF (2004) J Alloys Compd 374:320–324
27. Rocha GB, Freire RO, Júnior NBC, de Sá GF, Simas AM (2004) Inorg Chem 43:2346–2354
28. da Costa NB, Freire RO, dos Santos MAC, de Mesquita ME (2001) J Mol Struct (THEOCHEM) 545:131–135
29. de Mesquita ME, Júnior SA, Oliveira FC, Freire RO, Júnior NBC, de Sá GF (2002) Inorg Chem Commun 5:292–295
30. Malta OL, Gonçalves e Silva FR (1998) Spectrochim Acta, Part A 54:1593–1599
31. Stewart JJP (1993) MOPAC 93.00 Manual. Fujitsu Ltd, Tokyo, Japan
32. Freire RO, Rocha GB, Albuquerque RQ, Simas AM (2005) J Lumin 111:81–87
33. Malta OL, Gonçalves e Silva FR, Longo RL (1999) Chem Phys Lett 307:518–526
34. Gonçalves e Silva FR, Menezes JFS, Rocha GB, Alves S Jr, Brito HF, Longo RL, Malta OL (2000) J Alloys Compd 303:364–370
35. Ridley JE, Zerner MC (1976) Theor Chim Acta 42:223–236
36. Zerner MC, Loew GH, Kirchner RF, Mueller-Westerhoff UT (1980) J Am Chem Soc 102:589–599
37. Zerner MC (1990) ZINDO manual. QTP, University of Florida, Gainesville, FL
38. Rocha GB, de Mesquita ME, Simas AM, de Sá GF (1999) Mater Sci Forum 315:400–406